

# Nuances of Topological Superconductivity in Sr intercalated $\text{Bi}_2\text{Se}_3$ and Exceptional Magneto-resistance in Weyl semimetal NbP

---

**Satyabrata Patnaik**

**Jawaharlal Nehru University, New Delhi**

Collaborators : **Dr. Pabitra Biswas (ISIS, RAL, UK)**  
**Dr. Tanmoy Das (IISc, Bangalore)**  
**Dr. Goutam Sheet (IISER, Mohali)**

Students involved: **Dr. Prakriti Neha ,**  
**Dr. Shruti , Dr. Vishal Maurya, Dr. Sudesh**  
**Mr. Pawan Kumar, Mr. K.S. Jat, Mr. Vipin Nagpal**

---

***Geometric Phases in Optics and Topological Matters***

ICTS, January 21-24, 2020



*School of Physical Sciences, JNU, New Delhi*

***A reasonable man adapts himself to the society.  
An unreasonable man persists in trying, through his ways and  
means, till the society adopts him. Therefore, all progress  
depends on the unreasonable man.***

**GBS**



# Superconductivity and magneto-resistance in the shadow of Topological phases of Quantum Matter

---

1. P. Neha, P. Biswas, T. Das and S. Patnaik, **Phys. Rev. Materials** 3, 074201 (2019).
  2. Shruti, V. K. Maurya, P. Neha, P. Srivastava, and S. Patnaik, **Phys. Rev. B**, 92, 020506 (2015).
  3. Sirohi, A., Das, S., Neha, P., Jat, K.S., Patnaik, S., Sheet, G., **Phys. Rev. B**, 98, 094523 (2018).
  4. P. Kumar, Sudesh and S. Patnaik, **J. Phys. Commun.** 3, 115007 (2019).
  5. Sudesh, P. Kumar, P. Neha, T. Das, and S. Patnaik, **Scientific Reports** | 7:46062 | (2017).
- 

## Funding Acknowledgement:

**DST FIST, DST PURSE, and SERB EMR/2016/003998**

# Plan of the talk

---

1. Brief introduction to topological quantum matter
2. New superconducting systems based on chalcogenides
3. Superconductors derived from topological insulators
4. Pairing state in Sr-Bi<sub>2</sub>Se<sub>3</sub>; a Muon Spin Rotation study
5. Origin of exceptional magneto-resistance in NbP & TaSb<sub>2</sub>

# Superconductivity in Chalcogenides

---

Superconductors based on “chalcogens” : Sulfur (S), Selenium (Se) and Tellurium (Group 6A, co-member of O, Po)

Initial importance: Ternary Chevrel Phases

$M\text{Mo}_6\text{X}_8$  (X = Chalcogen, M can be metal/rare earth)

Record for highest  $H_{c2}$  among low  $T_c$  superconductors :  $\text{PbGd}_{0.2}\text{Mo}_6\text{S}_8$ ,  
( $T_c \sim 15\text{K}$ ,  $H_{c2} \sim 60\text{ T}$ )

Hydrogen sulphide ( $\text{H}_3\text{S}$ ) compound that shows superconductivity at 203 K under a pressure of 155 Gpa. [A. P. Drozdov et. al, Nature 525, 73-76 (2015)]


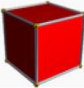

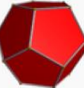

$$k_B T_c = 1.13 \hbar \omega_D \exp [-1/V N(E_F)]$$


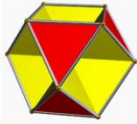
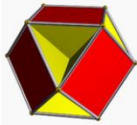



# Euler Characteristics is a topological invariant

A number that describes a shape or structure regardless of the way it is bent

$$\chi = V - E + F$$

Name	Image	Vertices $V$	Edges $E$	Faces $F$	Euler characteristic: $V - E + F$
Tetrahedron		4	6	4	2
Hexahedron or cube		8	12	6	2
Octahedron		6	12	8	2
Dodecahedron		20	30	12	2
Icosahedron		12	30	20	2

Name	Image	Vertices $V$	Edges $E$	Faces $F$	Euler characteristic: $V - E + F$
Tetrahemihexahedron		6	12	7	1
Octahemioctahedron		12	24	12	0
Cubohemioctahedron		12	24	10	-2
Great icosahedron		12	30	20	2

# Topology

**Gauss-Bonnet Theorem:** connects the geometry (*curvature*) of objects to their topology.

- For a closed surface  $M$ :

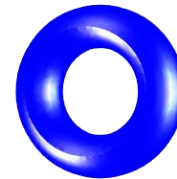
$$\int_{\mathcal{M}} K dA = g \quad g : \text{Integer}$$

$$\int K(\text{Dolphin}) = \int K(\text{Cow}) = \int K(\text{Sphere}) = 0$$

No. of hole =  $g = 0$

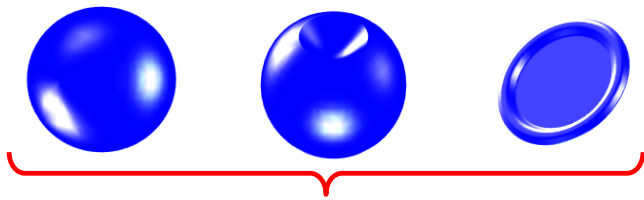
$$\int K(\text{Donut}) = \int K(\text{Mug}) = 1$$

No. of hole =  $g = 1$

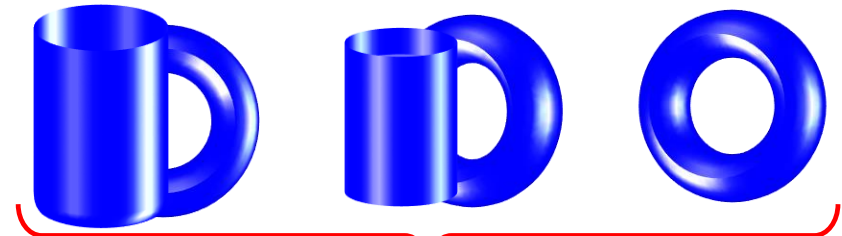


Topologically equivalent

# Topology and Insulators



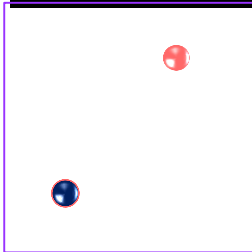
No. of hole = 0



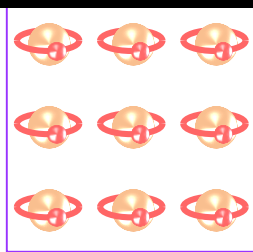
No. of hole = 1

Insulators are topologically equivalent if they can be continuously deformed into one another without closing the energy gap.

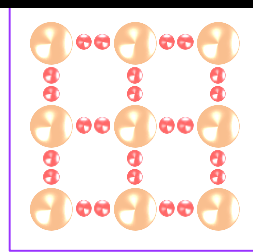
Dirac vacuum



Atomic insulator (Ar)



Covalent insulator (Si)



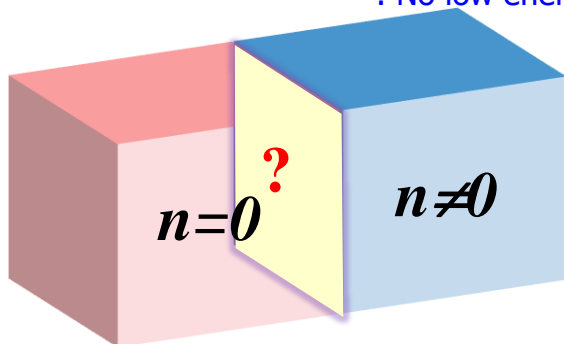
Topology of bulk band structure  
Chern number (TKNN 1982)

$$n = \frac{1}{2\pi i} \int_{BZ} d^2\mathbf{k} \cdot \langle \nabla_{\mathbf{k}} u(\mathbf{k}) | \times | \nabla_{\mathbf{k}} u(\mathbf{k}) \rangle = \text{Integer}$$

= 0, trivial insulator

= 1, 2, 3... ?

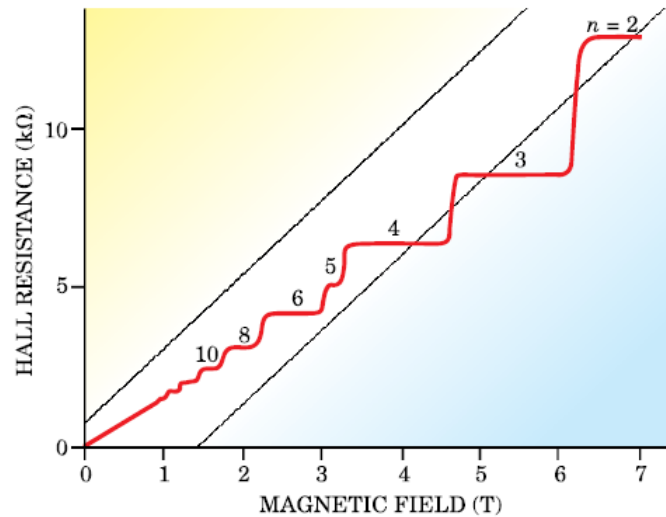
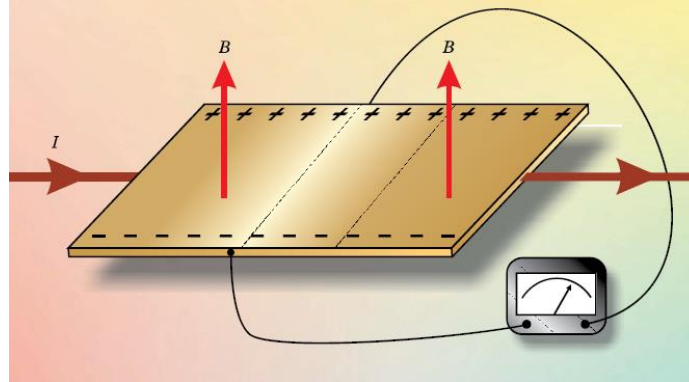
Characterized by energy gap: Does not conduct electricity  
: No low energy electronic excitations



Are there “topological phases” that are not adiabatically connected to the trivial insulator (i.e. the vacuum/covalent insulator)?



# Quantum Hall effect

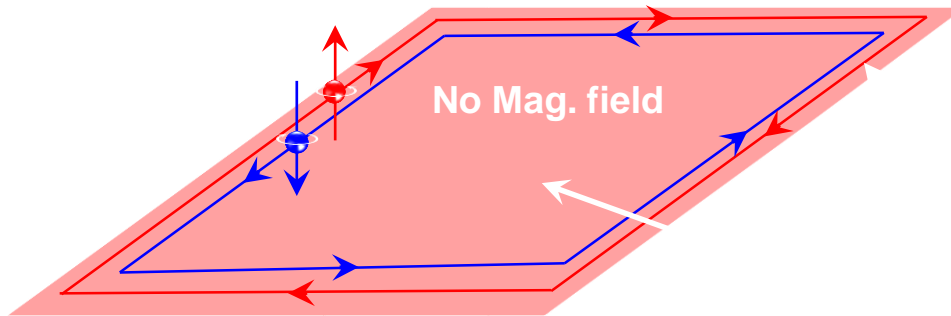


S C Zhang, Physics 1, 6 (2008)  
J. E. Avron, Physics Today (2003)

# Quantum Spin Hall effect; 2D Topological Insulators

Theoretical prediction (Kane and Mele 2005)

Simplest version: 2 copies of QHE



Unstoppable

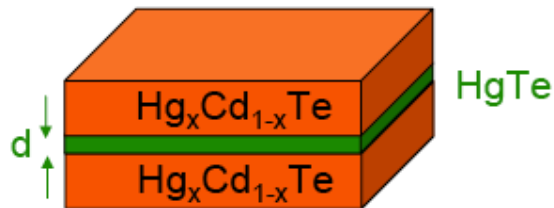


No U-turn



Insensitive  
to disorder

HgCdTe Quantum Well

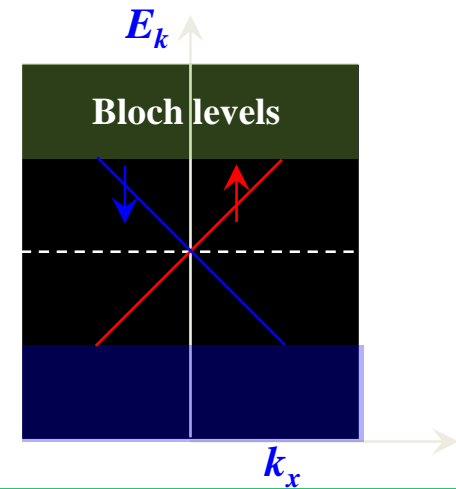


Slide from Dr. Rajiv Batabyal

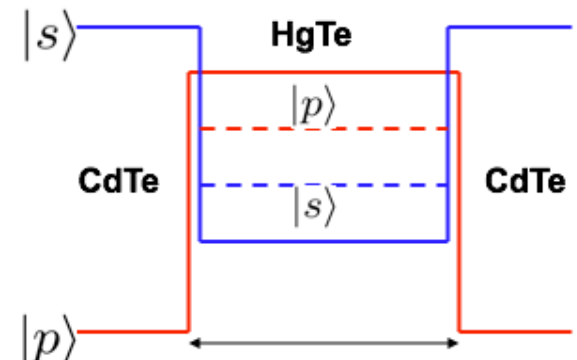
$$P|\psi_n(\Gamma_i)\rangle = \xi_n(\Gamma_i)|\psi_n(\Gamma_i)\rangle$$

$$\xi_n(\Gamma_i) = \pm 1$$

$$(-1)^{\nu} = \prod_{i=1}^4 \prod_n \xi_{2n}(\Gamma_i)$$



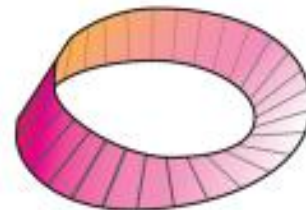
protected  
by time reversal symmetry



# Topological Quantum Matter

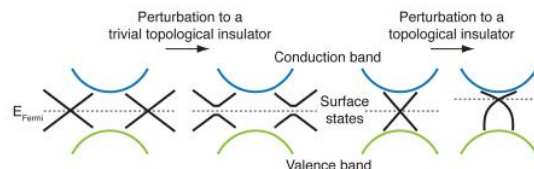
---

1. Integer and fractional quantum Hall effect have taught us that there is a new organizational principle at play. The edge current persists even in the presence of impurities. (Time reversal symmetry broken state)
2. In Topological insulators (e.g.  $\text{Bi}_2\text{Se}_3$ ) strong spin-orbit coupling plays the role of external magnetic field of QHE (Time reversal symmetry invariant state).



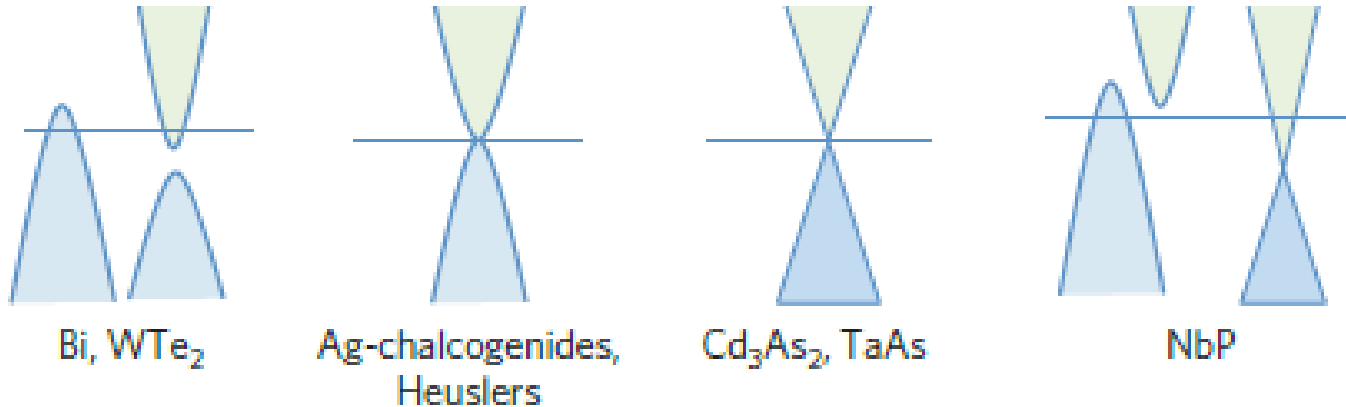
# What is special about Topological insulators?

1. Dangling bond or special organization of atoms in 2D can give rise to surface states within the forbidden gaps of an insulator. These are fragile states that depend on surface chemistry.
2. In contrast topological surface states are protected and their existence does not depend on how the surface is cut or on impurity at the surface.
3. In essence, their Hamiltonian is invariant under small perturbation.
4. Graphene is topologically trivial whereas  $\text{Bi}_{1-x}\text{Sb}_x$  is topologically protected.



# Weyl Semimetals

1. Weyl and Dirac semimetals are 3D analogues of Graphene. There is a band crossing point with linear dispersion at the Fermi level.
2. Ultrahigh mobilities and exceptional magnetoresistance are reported in these materials.



# SdH Oscillations and Berry Phase

---

**Shubnikov–de Haas effect (SdH)** is an oscillation in the electrical resistivity which is a macroscopic manifestation of the inherent quantum mechanical nature of matter

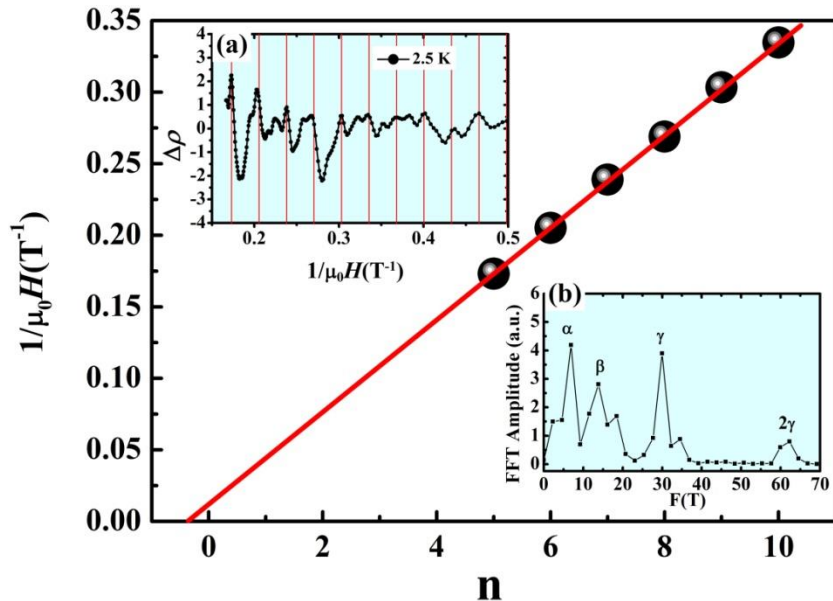
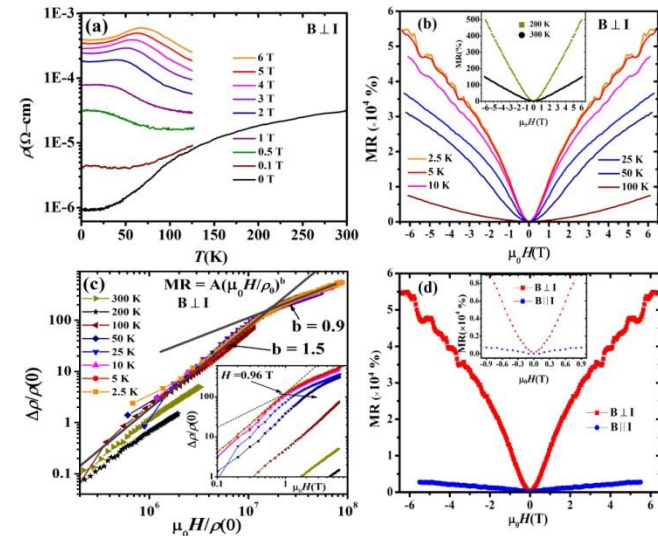
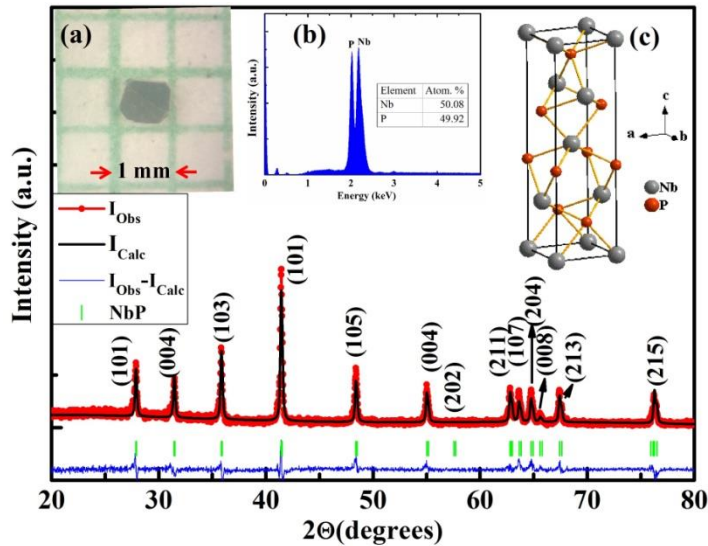
Free electrons in conduction band behave like harmonic oscillator whose oscillation period is proportional to external field.

As the magnetic field increases, the LL start crossing the Fermi level that depopulates the electrons and resistivity decreases.

Mean charge transport averaged over many cycles is quantized. Chern numbers reflect this quantization of averages.

Phase accumulated to wave function relates to Berry Phase

# Trivial Berry Phase and absence of Chiral anomaly In Weyl semimetal NbP



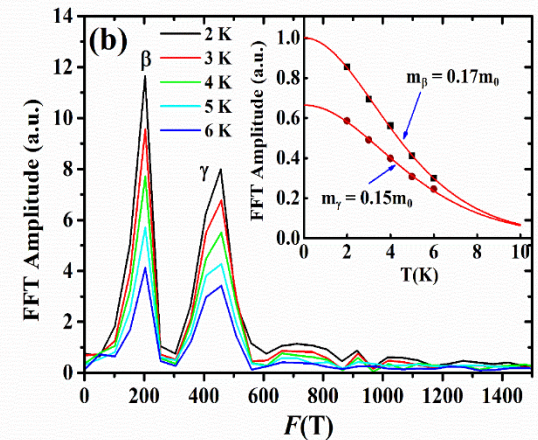
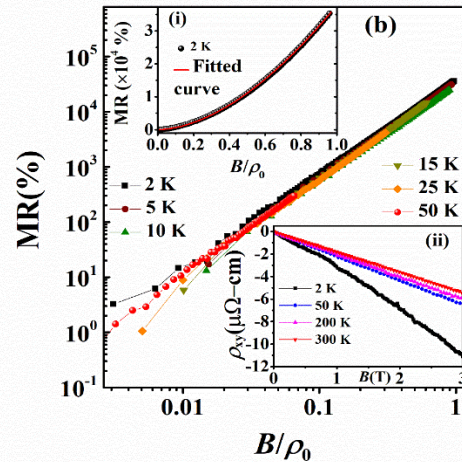
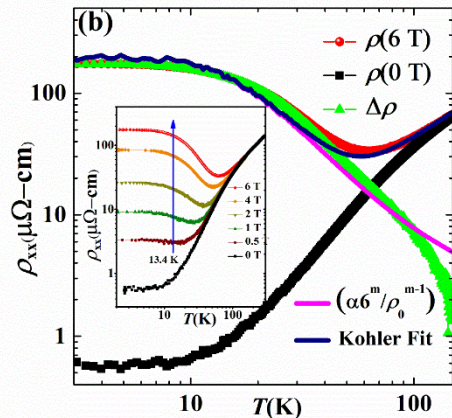
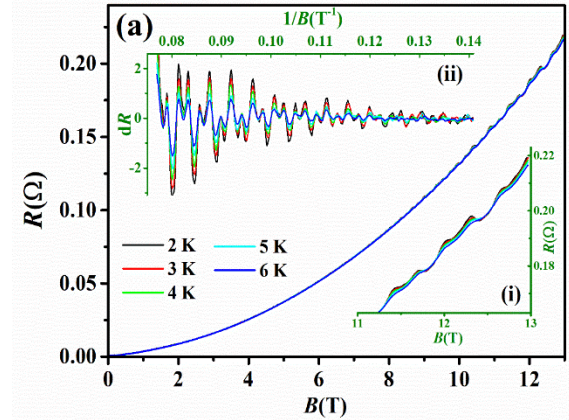
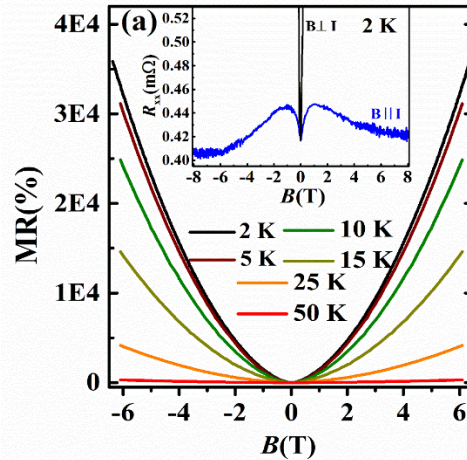
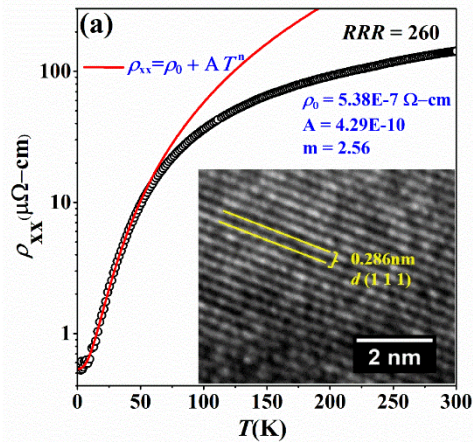
$$\Delta\rho/\langle\rho(0)\rangle = A(T, \mu_0 H) \cos\left[2\pi\left(\frac{F}{\mu_0 H} - \gamma + \delta\right)\right]$$

$$F = (\Phi_0 / 2\pi^2) A_F$$

$$\gamma = \frac{1}{2} - (\Phi_B / 2\pi) + \delta$$

No evidence for chiral anomaly was seen; Weyl points are far away from Fermi level and weak disorder

# Magnetic field-induced resistivity upturn and exceptional magneto-resistance in semimetal TaSb<sub>2</sub> (P. Kumar, J. Phys. Commun. 3, 115007 (2019))

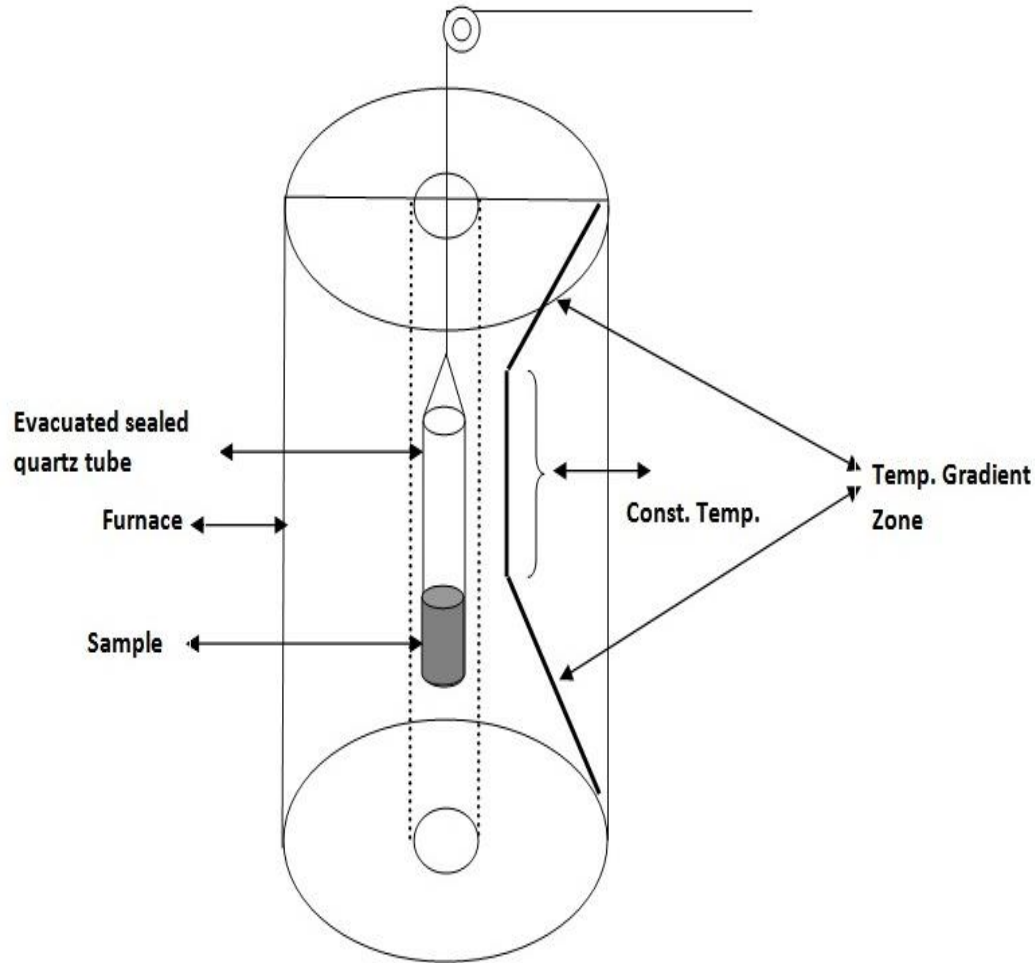
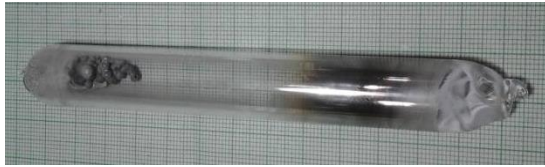


Topological superconductors: Sr and Nb intercalated Bi<sub>2</sub>Se<sub>3</sub>, BiPd, Sn<sub>1-x</sub>In<sub>x</sub>Te

Dirac/Weyl Semimetals : NbP, TaP, TaSb<sub>2</sub>, Bi<sub>1-x</sub>Sb<sub>x</sub>, ZrSi (S/Te/Se), MoP<sub>2</sub>, WP<sub>2</sub> and TaIrTe<sub>4</sub>



# Sample Preparation : Modified Bridgmann Technique



# Pairing Symmetry in superconductors

❖ A superconducting wave function has both spin and orbital (spatial) components.

❖ Spin component can be in a singlet state (Cooper pairs of opposite spin ( $\uparrow\downarrow$ )) or in a triplet state (Cooper pairs of the same spin ( $\uparrow\uparrow$ )).

❖ Fermions obey anti-symmetric exchange  $\Rightarrow$  If spin part of the wave function is anti-symmetric (Singlet spin state), orbital part is even i.e.  $L = 0$  (s-wave), 2 (d-wave). If spin part is symmetric (Triplet spin state), orbital part is to be odd i. e.  $L=1$  (p-wave), 3 (f-wave)

❖ Spatial part of superconducting Order Parameter is defined by a complex wave function  $\psi(\mathbf{k}) = \Delta(\mathbf{k}) e^{i\phi(\mathbf{k})}$  where  $\Delta(\mathbf{k})$  is the magnitude of the superconducting energy gap and  $\phi(\mathbf{k})$  is the phase of the order parameter.

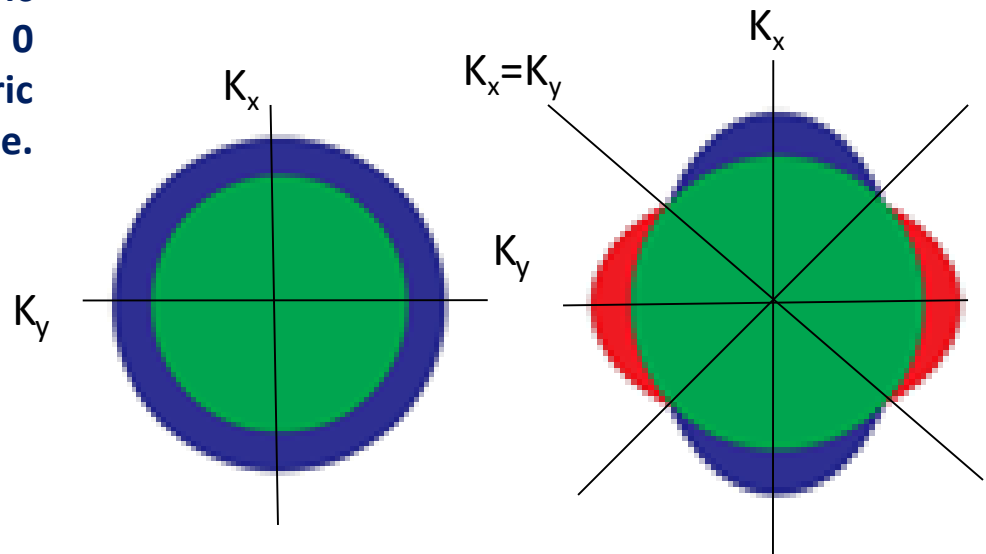
For a s-wave symmetry

$$\Delta = \Delta_0$$

For a  $d(x^2-y^2)$  symmetry,

$$\Delta(\mathbf{k}) = \Delta_0 |\cos(k_x a) - \cos(k_y a)|, \quad a \text{ is lattice constant}$$

The gap vanishes for  $|k_x| = |k_y|$  giving rise to four nodes along the diagonals in the Brillouin zone at the Fermi surface.



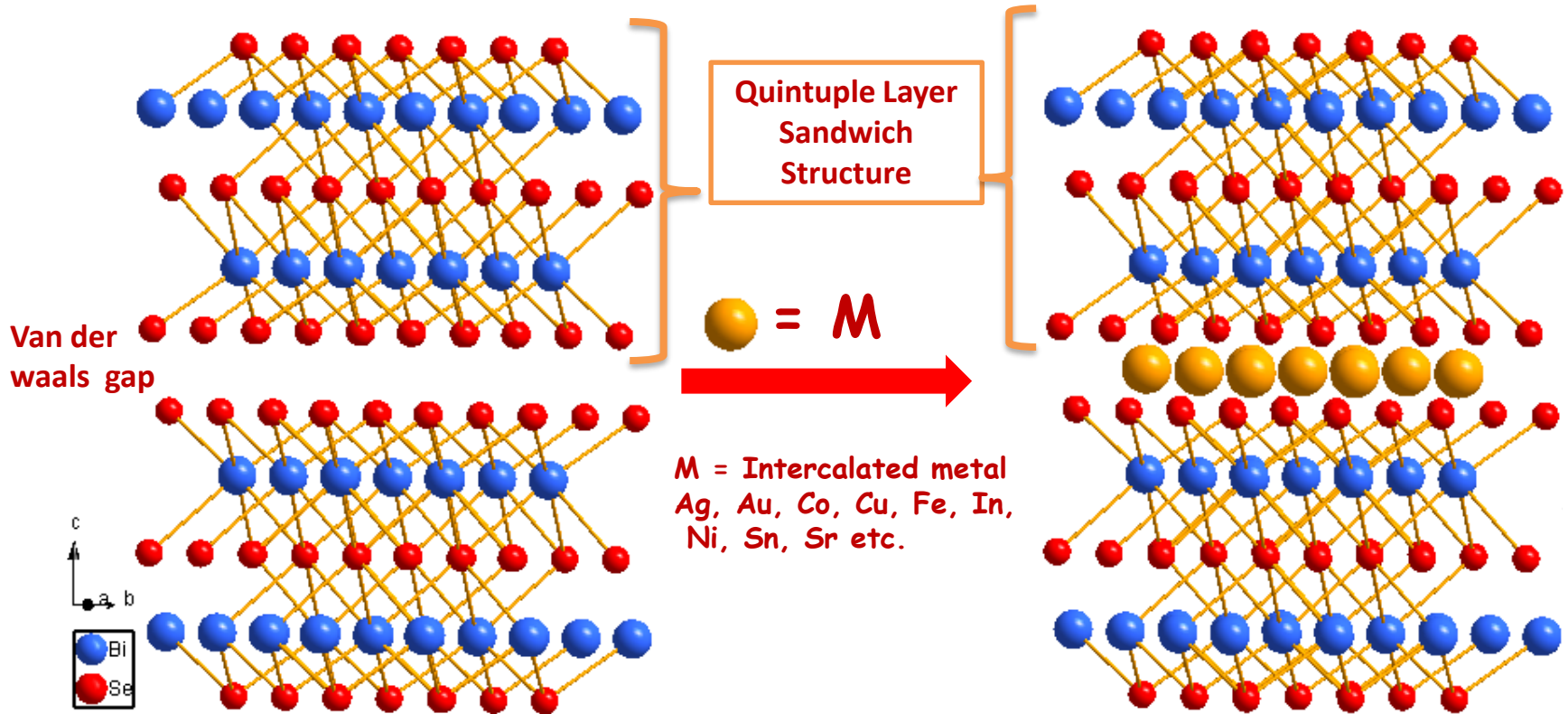
S-wave superconductor

d wave ( $x^2-y^2$ ) superconductor

# TRS pairing in Topological Superconductivity

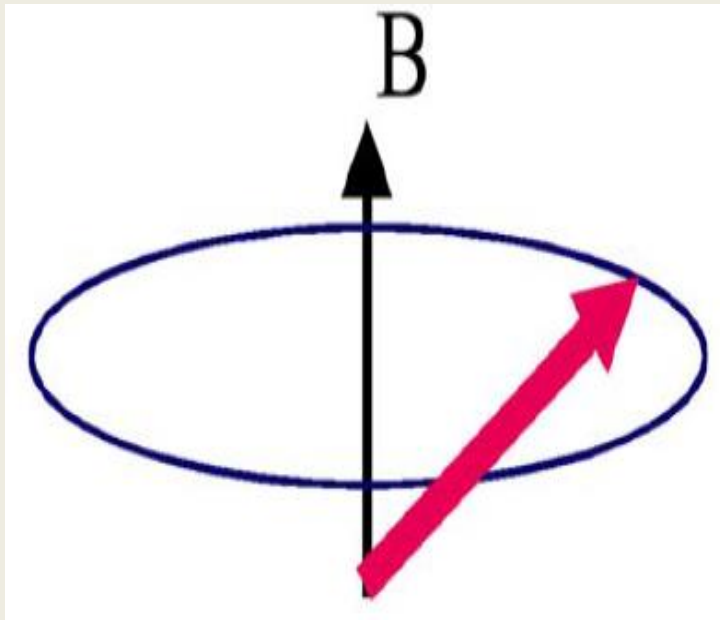
1. In 2D electron gases the Fermi surface splits into two counter helical pockets with TRSB expected.
2. Owing to Z2 topology surface states of Sr-Bi<sub>2</sub>Se<sub>3</sub> host only a single helical Fermi pocket.
3. Therefore only a singlet pair  $(\mathbf{k}\uparrow, -\mathbf{k}\downarrow)$  is allowed and the spin flip partner is absent.
4. The resulting pair wave function prescribes that the order parameter must be odd parity (Spinless (TRS) *p*-wave).

# Crystal Structure of $\text{Sr}_x\text{Bi}_2\text{Se}_3$



- $\text{Bi}_2\text{Se}_3$  belongs to the family of tetradymite compound with structural formula  $\text{A}_2\text{X}_3$  ( $\text{A} = \text{Bi}, \text{Sb}; \text{X} = \text{Se}, \text{Te}$ ).
- Crystal structure of  $\text{Bi}_2\text{Se}_3$  consists of five-layer units of Bi and Se hexagonal planes (quintuple), stacked along the c-axis with atomic order Se–Bi–Se–Bi–Se, and form rhombohedral lattices (space group R-3m) in which the unit cell is composed of three quintuple layers. The units are stacked on the top of each other and are weakly bonded by the van der Waals forces.
- $\text{Bi}_2\text{Se}_3$  is a popular material for thermoelectric studies. Recently  $\text{Bi}_2\text{Se}_3$  has emerged as one of the prime candidates for the study of topological surface states.

# Muon Spectroscopy



- Mass:  $m = 105.658 \text{ MeV}/c^2$
- Charge:  $+e$
- Spin :  $s = \frac{1}{2}$
- Magnetic moment:  $\mu = 3.18 \mu_p$
- Life time:  $\tau_\mu = 2.19714 \mu\text{s}$

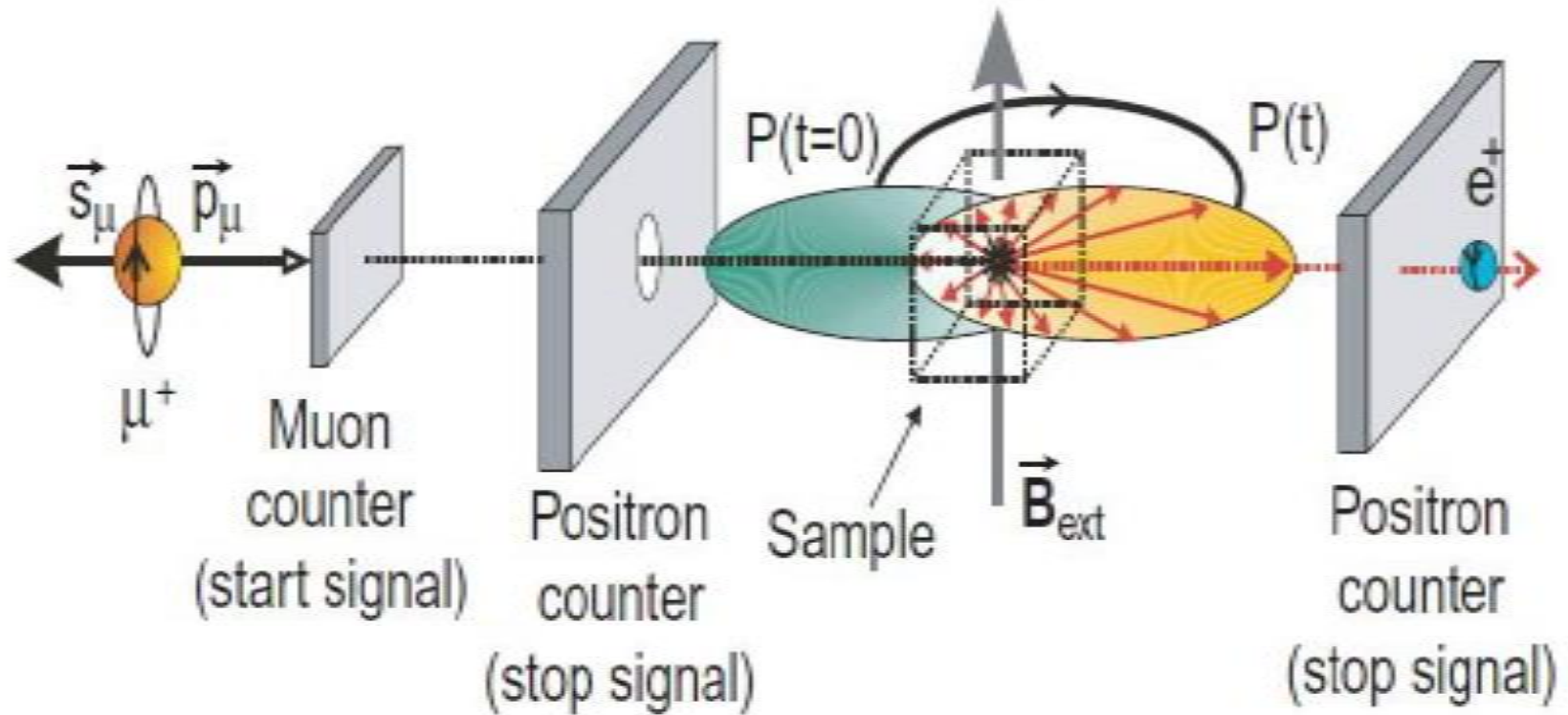
- The muon technique involves implanting 100% spin-polarised  $S=\frac{1}{2}$  positive muons into a material where they act as a local probe.
- The implanted muon precesses in local magnetic environment and then decays into positrons in  $2.2 \mu\text{s}$

$$\mu^+ = e^+ + \nu_\mu + \bar{\nu}_e$$

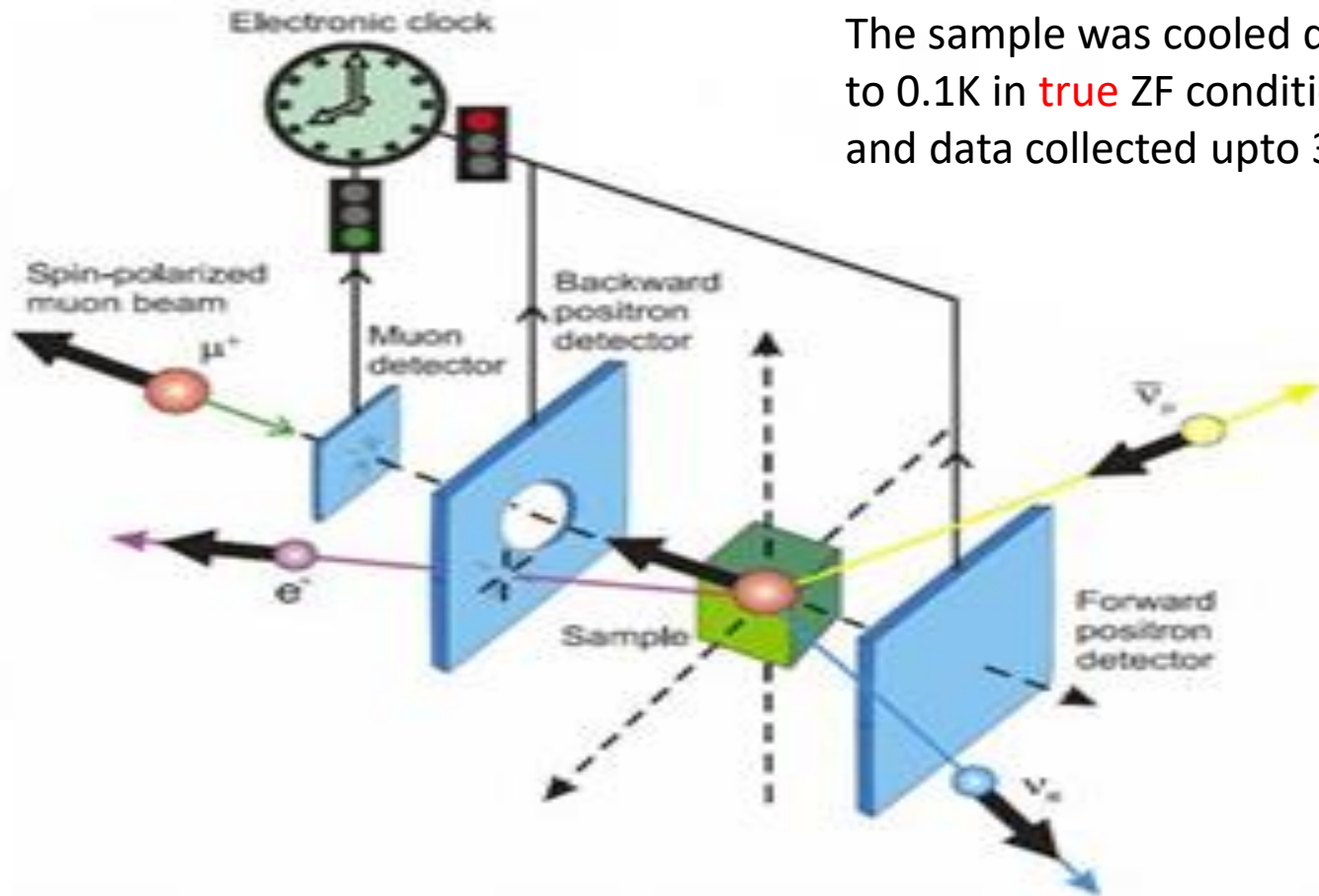
$$\left[ A(t) = \frac{N_F(t) - \alpha N_B(t)}{N_F(t) + \alpha N_B(t)} \right]$$

The decayed positron carry that information into detectors placed in the forward and backward direction. The asymmetry parameter is the normalized difference function between the positrons recorded in the forward detector and backward detector. The resolution of  $\mu\text{SR}$  is  $\sim 10 \mu\text{T}$

# Muon Spectroscopy Set Up



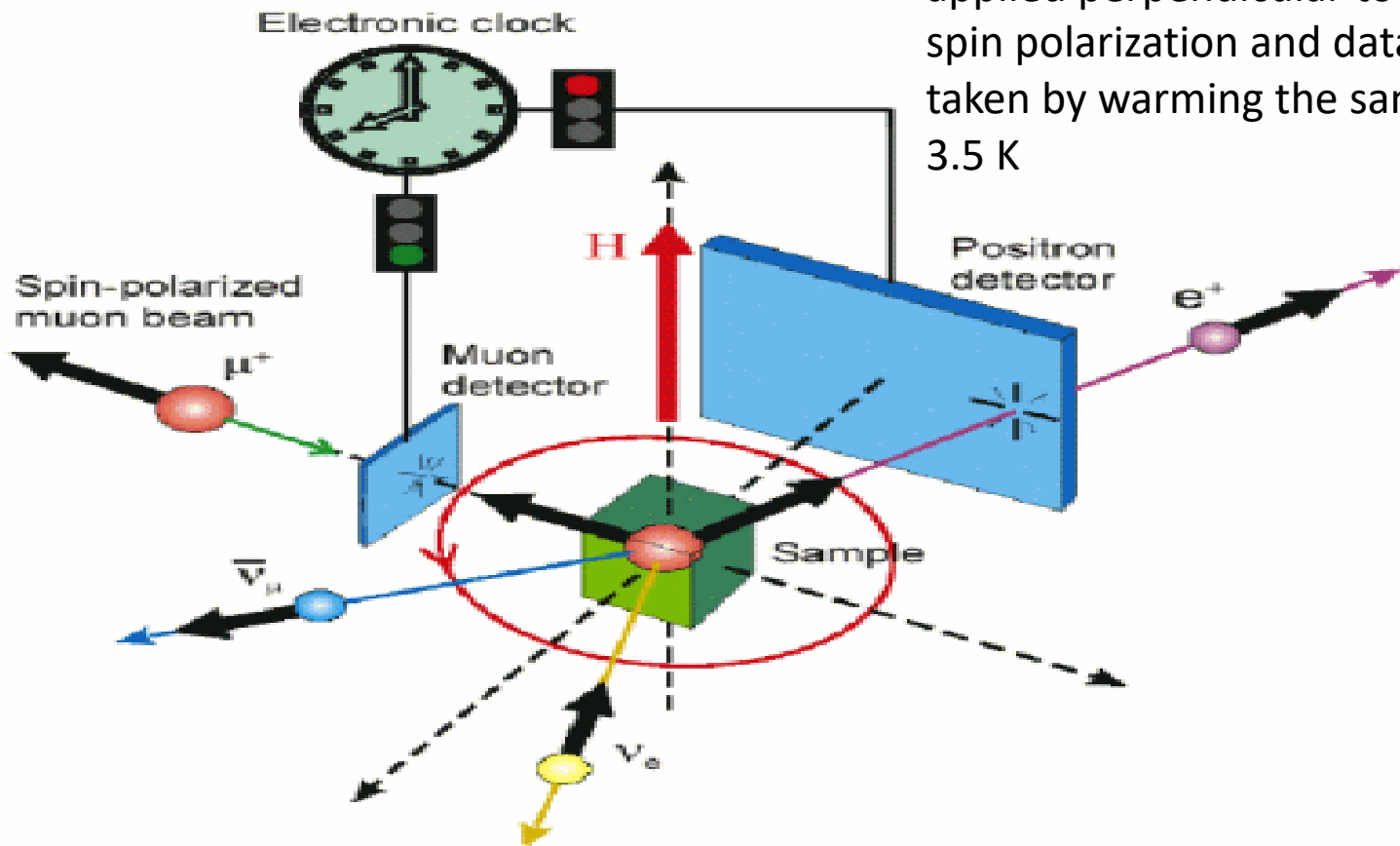
# Zero Field Muon Spectroscopy



The sample was cooled down to 0.1K in **true** ZF condition and data collected upto 3.7 K

# Transverse Field Muon Spectroscopy

The sample is cooled down to 0.09K in a magnetic field of 10mT applied perpendicular to muon spin polarization and data are taken by warming the sample to 3.5 K





# Zero-Field[ZF] $\mu$ SR

- The ZF  $\mu$ SR data taken at 0.1K and 3.7K for  $\text{Sr}_{0.1}\text{Bi}_2\text{Se}_3$  is best fitted for static Gaussian Kubo Toyabefunction multiplied by an exponential factor and decay rates  $a$  and  $\Lambda$ .
- $A(t) = A(0)G_{KT}(t) \exp(-at) + A_{bg}$  where,
- $$G_{KT} = \left[ \frac{1}{3} + \frac{2}{3}(1 - \Lambda^2 t^2) \exp\left[-\frac{\Lambda^2 t^2}{2}\right] \right]$$
- Here, Asymmetry variation shows breaking of Time Reversal Symmetry and presence of unconventional superconductivity

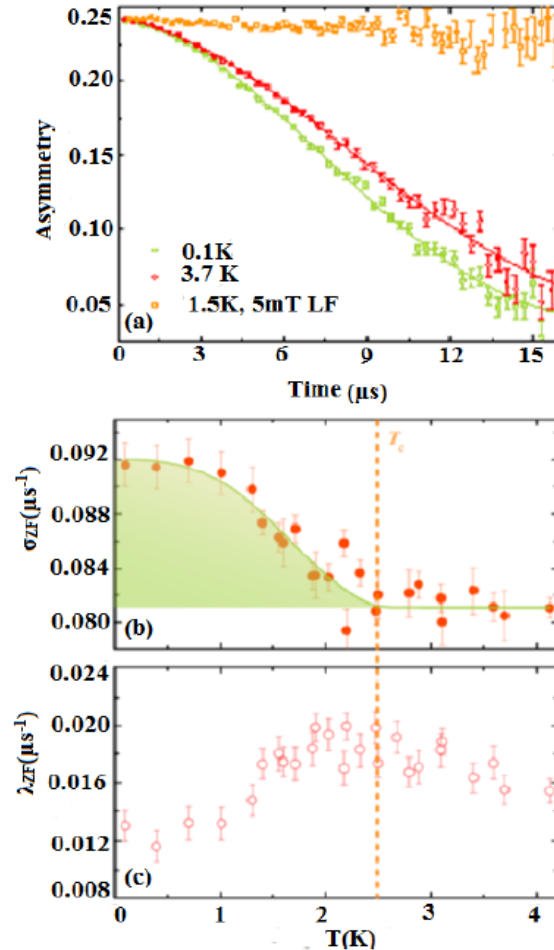


FIG. 1. (a) ZF- $\mu$ SR spectra collected at 0.1K and 3.7 K and LF data taken at 1.5 K applied field of 5mT. (b) Temperature variation of the muon spin relaxation rate  $\sigma_{ZF}$  above and below  $T_c$ . (c) Variation in  $\lambda_{ZF}$  with temperature also indicates existence of spontaneous field.

# Detection of pairing symmetry by Muon Spectroscopy

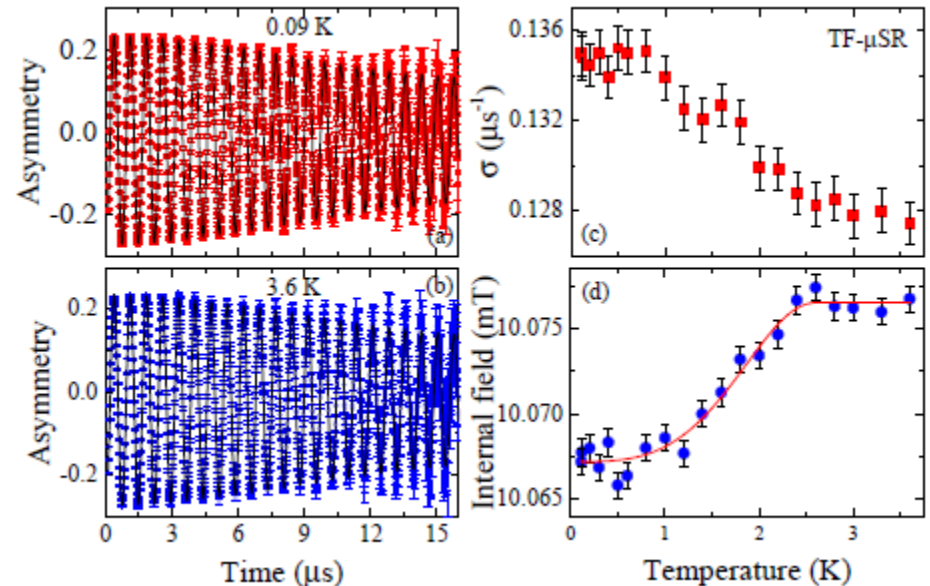
TF Muon spectra was taken at 0.09 K and 3.6 K respectively at 10mT applied field.

The asymmetry curve is fitted with the simple Gaussian type oscillatory distribution function

$$\begin{aligned}
 A(t) &= A(0)e^{-\sigma^2 t^2} \cos(\gamma_\mu B_{int} t + \varphi) \\
 &+ A_{bg} \cos(\gamma_\mu B_{bg} t + \varphi)
 \end{aligned}$$

where,  $\frac{\gamma_\mu}{2\pi}$ ,  $B_{int}$ ,  $B_{bg}$  are muon gyromagnetic ratio, muon frequencies from the muon precession signal and background signal respectively and  $\varphi$  is the phase angle.

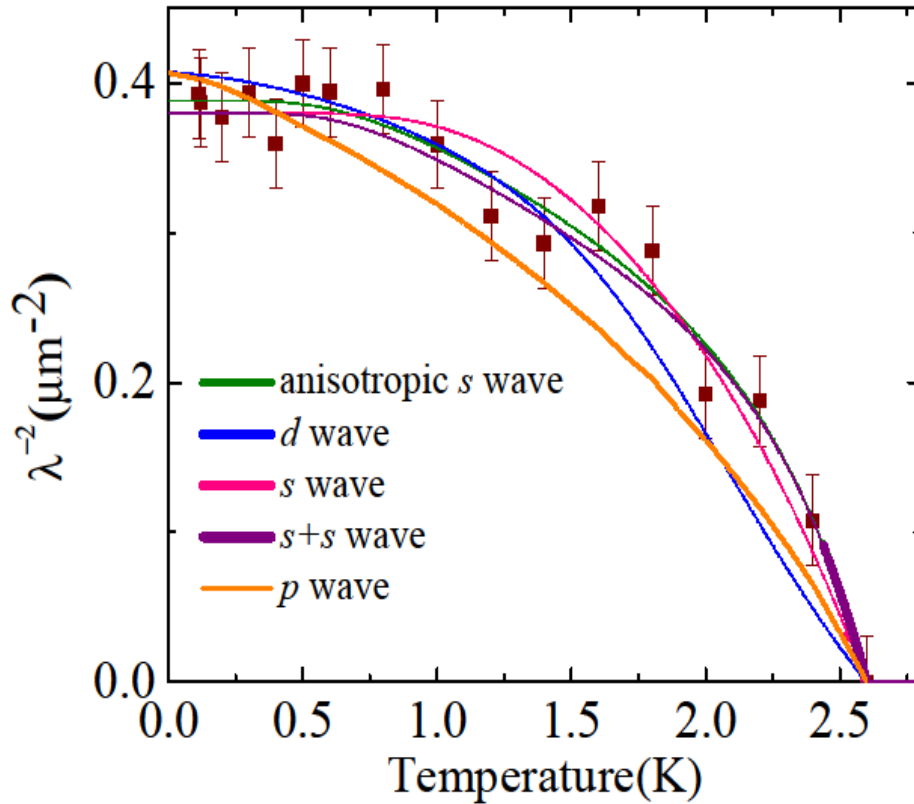
## Transverse-Field $\mu$ SR



Higher relaxation  $\sigma$  in SC state due to inhomogeneous field distribution

$$\sigma = \sqrt{\sigma_{sc}^2 + \sigma_{nm}^2} \quad \frac{\sigma_{sc}(T)}{\gamma_\mu} = 0.06091 \frac{\Phi_0}{\lambda^2(T)}$$

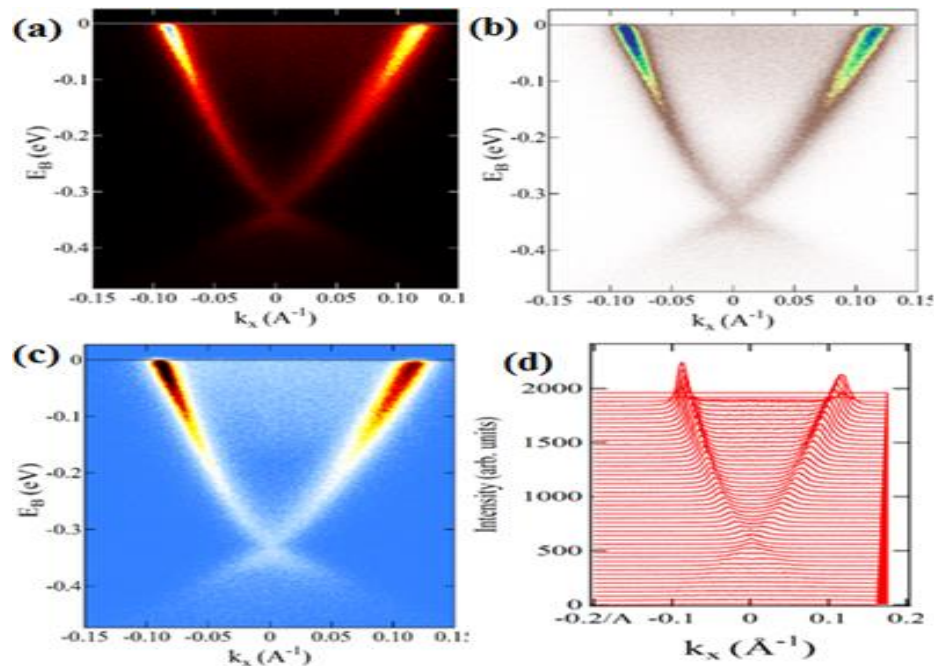
# Pairing Symmetry



Model	Gap value (meV)	$\chi^2$
<i>s</i> -wave	$\Delta=0.49(4)$	1.40
<i>s</i> + <i>s</i> -wave	$\Delta_1=0.7(3)$ , $\Delta_2=0.3(1)$ and $\omega = 0.58(8)$	1.06
anisotropic <i>s</i> -wave	$\Delta = 0.54(6)$ with $s = 0.6(2)$	1.02
<i>p</i> -wave	$\Delta=0.55(3)$	4.27
<i>d</i> -wave	$\Delta=0.4(1)$	3.53

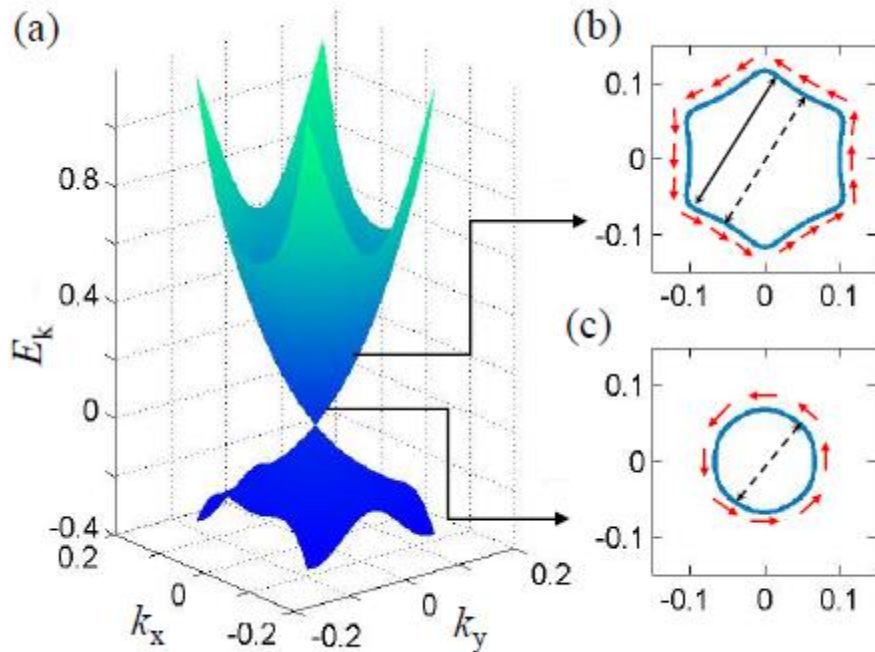
- The TF muon spectroscopy yields the presence of nodeless superconductivity
- The muon spectroscopy in ZF mode and TF mode yields coexistence of singlet and triplet.

# Surface states?



- Low Meissner fraction
- ARPES shows Dirac features in Sr intercalated  $\text{Bi}_2\text{Se}_3$
- The muon spectroscopy probes surface states of grains with large penetration depth.

# Origin of TRSB and singlet –triplet mixing



- In  $\text{Sr}_{0.1}\text{Bi}_2\text{Se}_3$  chemical potential lies far above Dirac Point.
- Spin-momentum locking weakens as we move away from Fermi level due to hexagonal warping and higher order SOC.
- Away from the Dirac point the Fermi surface becomes snowflake type and spin texture becomes anisotropic.

Single helical surface state of a 3D topological insulator in the  $k_x$  -  $k_y$ -plane. (b-c) Constant energy cuts close to the Dirac cone (b) and far from the Dirac cone (c). Red arrows show the corresponding spin alignments across the corresponding constant energy contours. Dashed arrow dictated the  $k$  and  $-k$  points in which spin is anti-parallel, while the solid arrows shows similar points where anti-parallel alignment of the spin is weakened due to higher order SOC and hexagonal warping effects.

# Conclusions

---

- **The ZF  $\mu$ SR spectroscopy measurement yields the presence of TRS breaking and indicates the presence of triplet Cooper pairing and unconventional superconductivity.**
- **The TF  $\mu$ SR spectroscopy measurements yields the presence of nodeless superconductivity.**
- **Such mixing of singlet and triplet pairing symmetry is understood as a consequence of hexagonal warping and higher order spin –orbit coupling terms.**

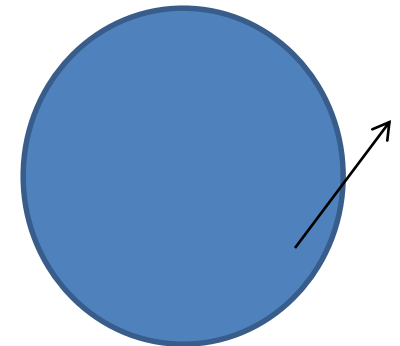
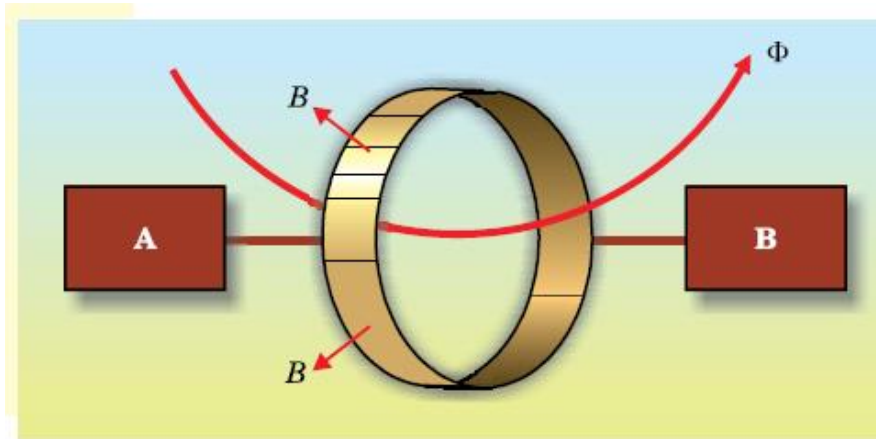
# Thank You

**Funding Acknowledgement:**

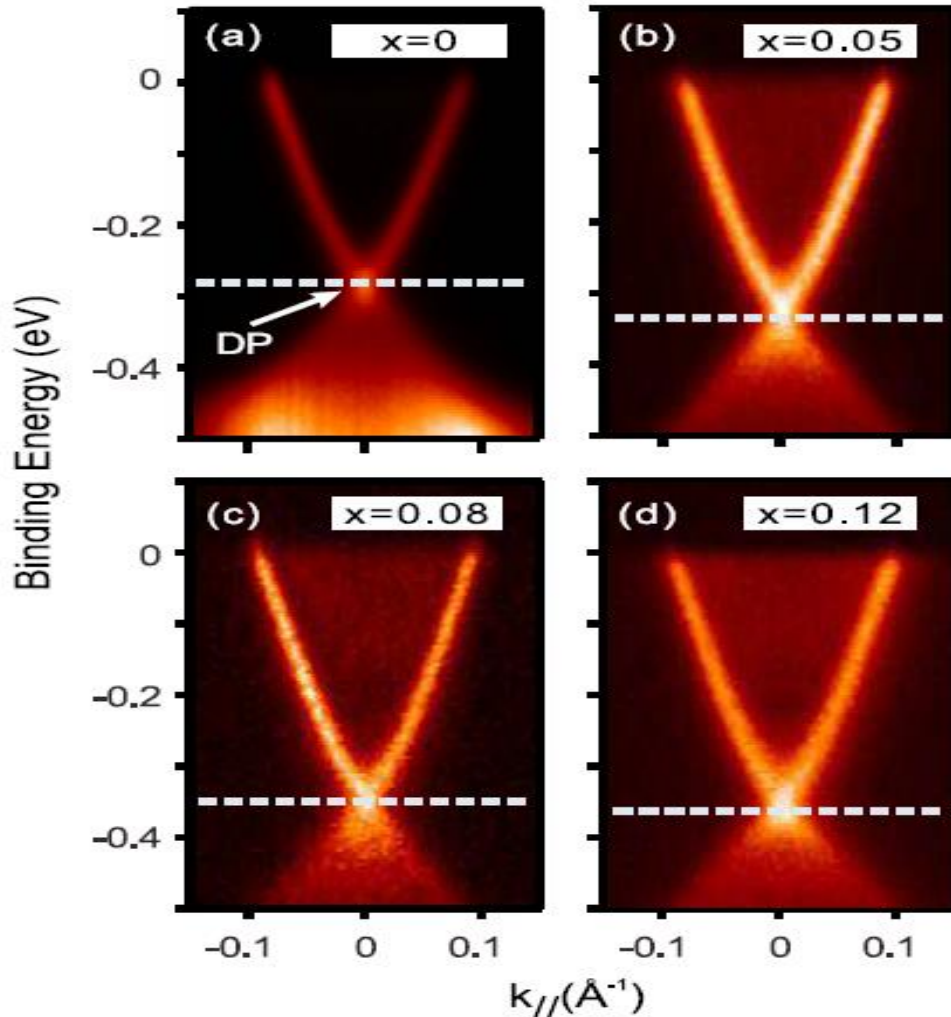
**DST FIST, DST PURSE and SERB EMR/2016/003998**

# Laughlin's Explanation

1. QHE is a Quantum pump.
2. Charge transported by one cycle of pump (one flux quantum) corresponds to units of Hall conductance steps.
3. Mean charge transport averaged over many cycles is quantized. Chern numbers reflect this quantization of averages.
4. Phase accumulated to wave function relates to Berry Phases







- The shift in Dirac point is observed on increasing the Sr doping percentage. The shift in Dirac point is due to change in chemical potential.

# Why is it hard to find applications using Superconductors?

- Temperature ?
- Difficult to make wires (granular , c-axis orientation )?
- Cost ?
- Vortex dynamics ?
- Irreversibility field

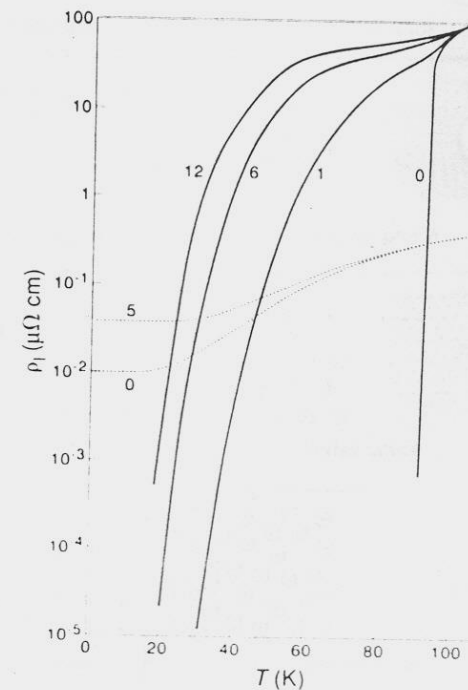
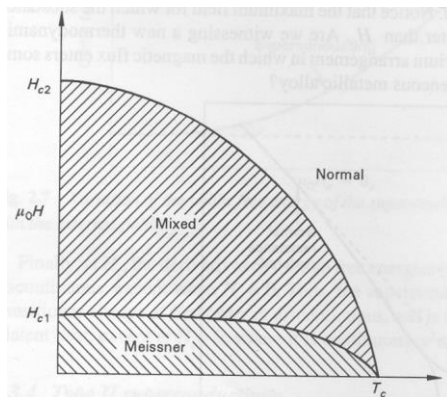
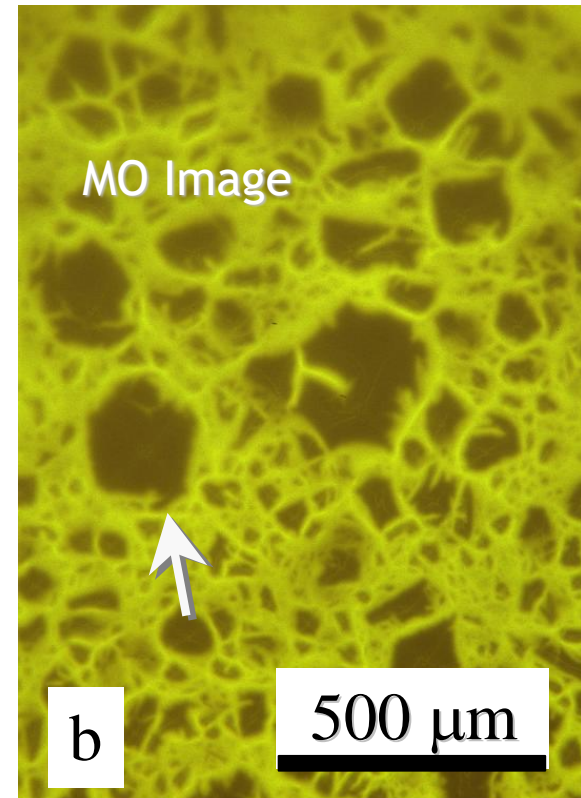
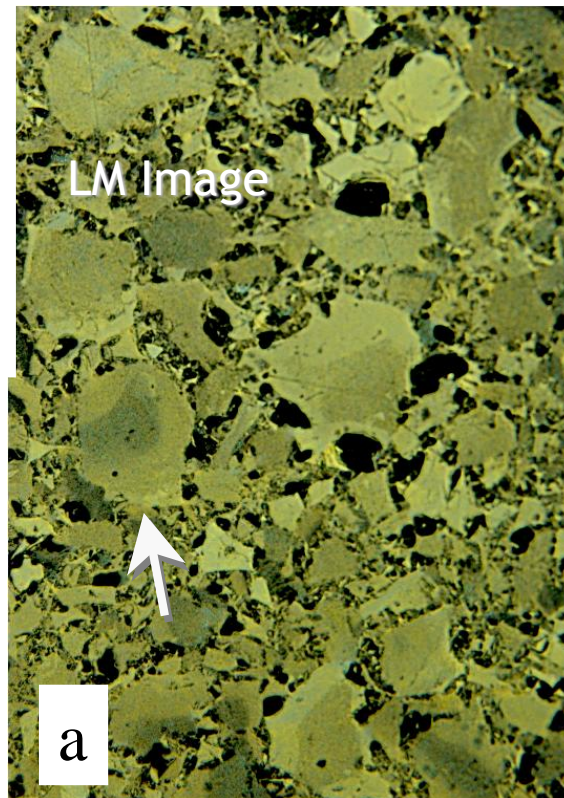
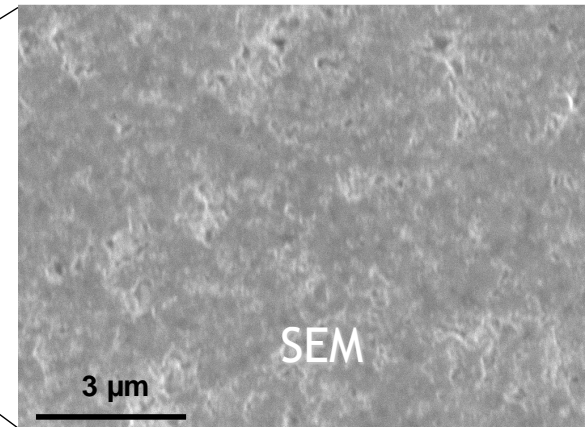
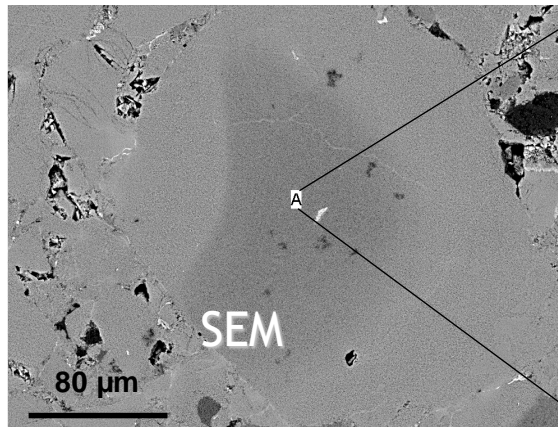
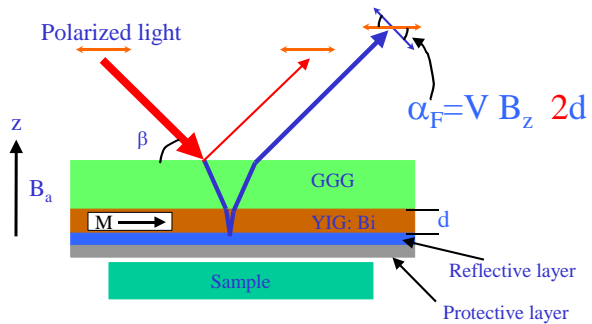


FIG. 1 The temperature ( $T$ ) dependence of the linear response resistivity,  $\rho_l = \lim_{J \rightarrow 0} \{E/J\}$ , where  $E$  is the electric field and  $J$  is the current density in the material. The solid curves are for  $\text{Bi}_2\text{Sr}_2\text{CaCu}_2\text{O}_{8-x}$  (BSCCO) and, for comparison, the dotted curves are for high-conductivity copper. Each curve is for a different magnetic field, indicated in tesla. Data are from refs 33-35. For low-temperature superconductors the drop in the resistivity remains fairly abrupt even in a magnetic field (as it is for BSCCO in zero field only).

Huse et al. Nature 553, 358 (1992)

# Bulk samples – connected GBs

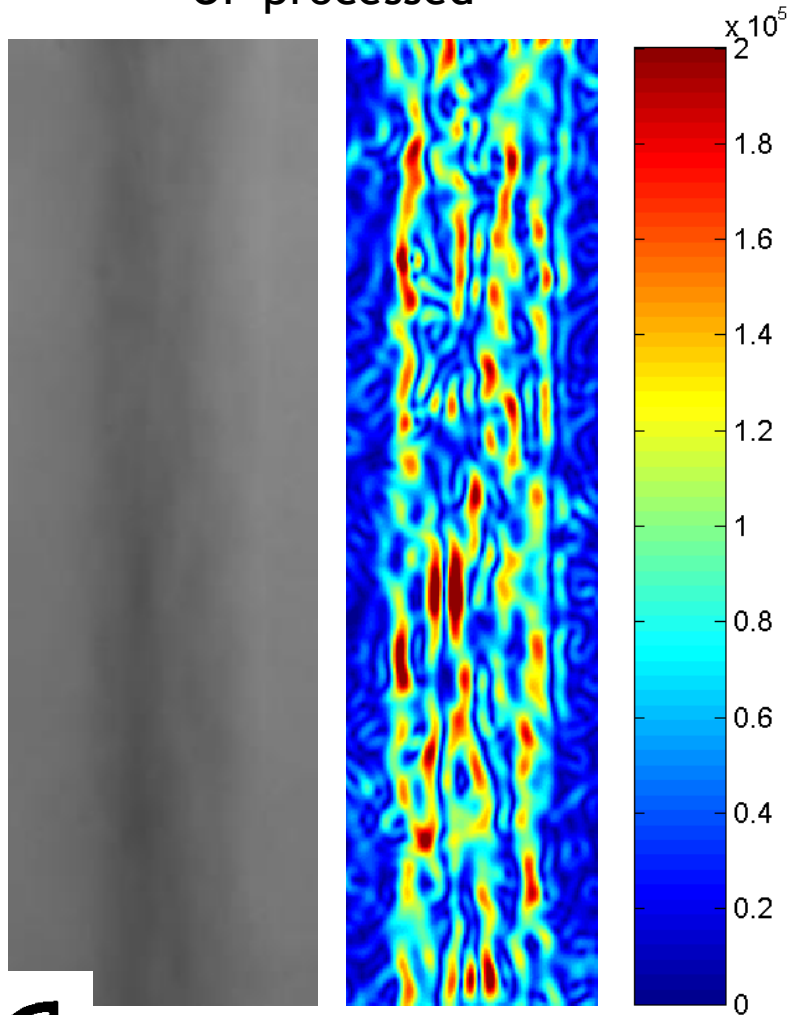
Schematic observation of MO picture by means of the magneto-optical double Faraday effect in reflective mode in YIG indicated film with in-plane magnetization



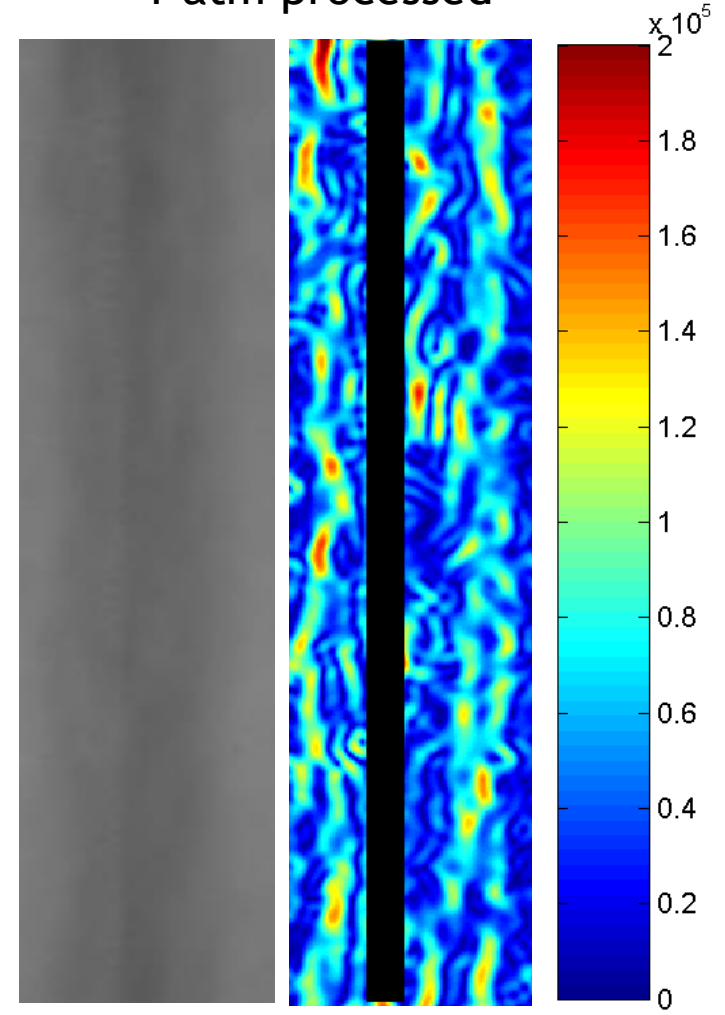
Nature 410, 186 ( 2001 ).

# OP and 1atm comparison ( 77K, 46mT )

OP processed



1 atm processed



Monocore sample width  $\sim 100\mu\text{m}$

School of Physical Sciences, JNU, New Delhi